Self-consistent calculations of the pair potential and the tunneling density of states in proximity contacts

Gerhard Kieselmann*
Physikalisches Institut der Universität Bayreuth, 8580 Bayreuth, Federal Republic of Germany
(Received 15 August 1986)

By the use of the quasiclassical theory, the pair potential and the tunneling density of states of a so-called proximity contact, i.e., a superconducting layer N of thickness a on top of a very thick superconducting substrate S, are self-consistently calculated. Special attention is given to N layers with a thickness of the order of the coherence length, in which case the pair potential deviates appreciably from a step. Free parameters in the numerical calculation are the film thickness a, the ratio of the Fermi velocities of the two metals, the ratio of their transition temperatures, and a potential strength that describes possible imperfections of the contact plane. The calculated density of states is compared with the approximate results obtained from the often-used step model for the order parameter. This model reproduces the rigorous numerical results reasonably well, provided the parameters of the step are properly adjusted.

I. INTRODUCTION

A variety of phenomena that are caused by the proximity effect between superconductors have been extensively studied over the years (see, e.g., Refs. 1–4). A theorist willing to describe such systems is confronted with the inherent inhomogeneity of the situation, which leads for instance to a spatially varying pair potential. In order to treat such problems, three different theoretical methods are available: the microscopic approach based on Green's functions, the Ginzburg-Landau theory, and the quasiclassical method. Microscopic Green's functions have been calculated only in the approximation of a steplike pair potential.[5–11] A large amount of numerical work would be needed to determine such a Green's function for more realistic pair potentials. For this reason, no self-consistent calculations of the pair potential of an inhomogeneous superconductor have yet been performed with the Green's-function technique. On the other hand, the Ginzburg-Landau approach is very well suited for tackling inhomogeneous systems, but it is only valid near the transition temperature. The quasiclassical theory based on so-called ξ-integrated or quasiclassical Green's functions closes the gap between the different approaches described above. It is not a microscopic theory, because its validity is restricted to a length scale that is large compared to the wavelength of the conduction electrons. On the other hand, it goes far beyond the Ginzburg-Landau theory. This method does not assume a small pair potential and is, in particular, valid at all temperatures. The basic equations of the theory have the character of transport equations and can, in general, be easily solved on a computer. This makes the theory in many cases more attractive than the microscopic approach.

In this article, I present self-consistent calculations of the pair potential and the tunneling density of states for the widely discussed proximity junctions[4] (see Fig. 1): a superconductor N of thickness a in electrical contact to a superconducting substrate S (following a standard notation for the layer and the substrate). I study, in particular, systems with thick layers (a approximately equals coherence length), where the pair potential deviates appreciably from a step function and standard Green's function methods[4,9] can no longer be applied. The conduction electrons are described, for simplicity, by a one-band model with an effective mass m^* and an effective Fermi velocity v_F^* as parameters; the Fermi surface is assumed to be spherical. The values for m^* and v_F^* may be different in both metals. Imperfections of the contact plane are accounted for by an interface potential with a potential strength V_s.

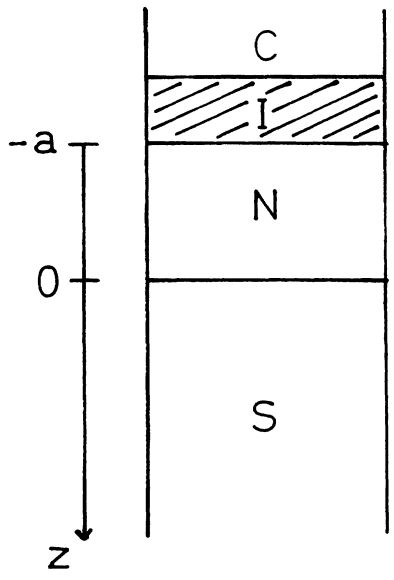

FIG. 1. Proximity junction C is the counterelectrode, I an insulating layer, N a superconducting or normal-conducting film of thickness a, and S the superconducting substrate.

Switching from a weak-coupling to a strong-coupling description is very easy within the framework of the quasiclassical theory: the quasiclassical equations formally remain the same, only the self-consistency equations for the self-energy parts change. Self-consistent calculations of the pair potential are indeed of comparable ease for both weak- and strong-coupling superconductors. Calculation of the tunneling density of states is a bit more involved in the strong-coupling case.

The quasiclassical theory is a convenient method for a rigorous, quantitative description of real proximity contacts. Previous work based on microscopic Green's functions relied on the model of a steplike pair potential. It has never been checked how the results change when this assumption breaks down, as is, for instance, the case for layer thicknesses $a \sim \xi$. A calculation which is free of uncontrolled approximations becomes important, if the theory is used to analyze experimental tunneling data for more basic material parameters such as, e.g., Fermi velocities, electronic mean free paths, or Eliashberg's spectral functions $\alpha^2 F(\omega)$.[12-22] In addition, tunneling data also carry information on Fermi-liquid parameters of the conduction electrons[23] and on properties of the interface (reflection coefficients, roughness[24]). All these effects can be incorporated in the quasiclassical formulation without difficulties.

In Sec. II the basic equations are introduced and a short analytical calculation of the tunneling density of states for the simple-step approximation of the pair potential is given. This calculation demonstrates that the quasiclassical theory is capable of reproducing familiar results without much effort. The self-consistent, numerical calculations for the pair potential and the tunneling density of states are presented and discussed in Sec. III. A special purpose of this article is to study the influence of self-consistency on the tunneling density of states. These calculations are done for pure systems in the weak-coupling limit. For comparison, I include a few strong-coupling results for the self-consistent pair potential. A summary is given in Sec. IV.

II. THE BASIC EQUATIONS

The quasiclassical propagator (also called the ξ-integrated Green's function) $\hat{g}(\hat{\mathbf{p}},\mathbf{R};\varepsilon_n)$ is connected to the microscopic Green's function $\hat{G}(\mathbf{p},\mathbf{R};\varepsilon_n)$ by

$$\hat{g}(\hat{\mathbf{p}},\mathbf{R};\varepsilon_n)=\hat{\tau}_3 \int d\xi_p \hat{G}(\mathbf{p},\mathbf{R};\varepsilon_n) . \tag{2.1}$$

where $\mathbf{R}$ and $\mathbf{p}$ denote the position and momentum variables, $\hat{\mathbf{p}}$ is the unit vector $\mathbf{p}/|\mathbf{p}|$, and $\hat{\tau}_{1,2,3}$ are the Pauli matrices in particle-hole space. (I use 2×2 Nambu matrices; they are indicated by a hat.) The integration is performed over the energy variable $\xi_p = v_F(p-p_F)$ along a path normal to the Fermi surface. The quasiclassical analog of the Gorkov equations reads

$$[i\tilde{\varepsilon}_n(\mathbf{R})\hat{\tau}_3-\hat{\Delta}_n(\mathbf{R}),\hat{g}(\hat{\mathbf{p}},\mathbf{R};\epsilon_n)]+iv_F\hat{\mathbf{p}}\nabla_R\hat{g}(\hat{\mathbf{p}},\mathbf{R};\varepsilon n)=0 \tag{2.2a}$$

with

$$\hat{\Delta}_n(\mathbf{R})=i\{\hat{\tau}_2 \mathrm{Re}[\tilde{\Delta}_n(\mathbf{R})]+\hat{\tau}_1 \mathrm{Im}[\tilde{\Delta}_n(\mathbf{R})]\} , \tag{2.2b}$$

where the diagonal and off-diagonal self-energies $\tilde{\varepsilon}_n(\mathbf{R})$ and $\tilde{\Delta}_n(\mathbf{R})$ are determined by the local Eliashberg equations [see (2.6)]. Within the framework of the strong-coupling theory, v_F is the bare Fermi velocity, i.e., $v_F=(1+\lambda)v_F^*$, where λ is the electron-phonon coupling constant. The solution of (2.2a) has to be normalized according to

$$[\hat{g}(\hat{\mathbf{p}},\mathbf{R};\varepsilon_n)]^2=-\pi^2 . \tag{2.2c}$$

The nomenclature and conventions used in this article are the same as in Ref. 23. Anyone interested in more details is referred to the original literature[25,26] and to Refs. 27 and 28.

The proximity system studied here is sketched in Fig. 1. It is translationally invariant with respect to the x and y directions, so that the spatial dependence of $\hat{g}$ reduces to a variation with z. Since the system carries no current, the pair potential can be chosen real and positive. Equation (2.2a) therefore reduces to

$$[i\tilde{\varepsilon}_n(z)\hat{\tau}_3-i\hat{\Delta}_n(z)\hat{\tau}_2,\hat{g}(\hat{\mathbf{p}},z;\varepsilon_n)]+iv_F(z)\hat{\mathbf{p}}\cdot\hat{\mathbf{z}}\partial_z\hat{g}(\hat{\mathbf{p}},z;\varepsilon_n)=0 \tag{2.3a}$$

with

$$v_F(z)=\begin{cases} v_{F,N}, & -a<z<0 \ \text{(metal } N\text{)}, \\ v_{F,S}, & 0<z \ \text{(metal } S\text{)} . \end{cases} \tag{2.3b}$$

$\hat{g}(\hat{\mathbf{p}},z;\varepsilon_n)$ has to fulfill the normalization condition (2.2c) and the following boundary or matching conditions.

(1) At the specularly reflecting outer wall ($z=-a$) the relation

$$\hat{g}(\hat{\mathbf{p}},-a;\varepsilon_n)=\hat{g}(\underline{\hat{\mathbf{p}}},-a;\varepsilon_n) \tag{2.4}$$

holds with $\underline{\hat{\mathbf{p}}}=\hat{\mathbf{p}}-2\hat{\mathbf{z}}(\hat{\mathbf{p}}\cdot\hat{\mathbf{z}})$; i.e., $\hat{g}$ is continuous along a classical flight trajectory.[29,30]

(2) $\hat{g}(\hat{\mathbf{p}},z;\varepsilon_n)$ is bounded everywhere.

(3) At the NS interface ($z=0$),

$$\hat{d}_N=\hat{d}_S , \tag{2.5a}$$

$$-i\pi\frac{1-R_z}{1+R_z}\left[\hat{s}_S\left[1-\frac{i}{2\pi}\hat{d}_S\right],\hat{s}_N\right]=\hat{d}_S\hat{s}_S^2 \tag{2.5b}$$

must be fulfilled[31,32] with the abbreviations

$$\hat{d}_k(\mathbf{p}_{||})=\hat{g}_k(\hat{\mathbf{p}}_{+,k},0)-\hat{g}_k(\hat{\mathbf{p}}_{-,k},0) \quad (k=N,S) , \tag{2.5c}$$

$$\hat{s}_k(\mathbf{p}_{||})=\hat{g}_k(\hat{\mathbf{p}}_{+,k},0)+\hat{g}_k(\hat{\mathbf{p}}_{-,k},0) \quad (k=N,S) ,$$

and

$$\hat{\mathbf{p}}_{\pm,k}=[\mathbf{p}_{||}\pm(p_{F,k}^2-p_{||}^2)^{1/2}\hat{\mathbf{z}}]/p_{F,k} . \tag{2.5d}$$

The subscripts N and S refer to the left-hand and the right-hand sides of the interface, respectively. $\mathbf{p}_{||}$ is a vector lying in the contact plane (see Fig. 2). R_z is the direction-dependent reflection coefficient. Its specific form depends, of course, on the chosen model for the metals and their common interface. In the weak-coupling calculations presented below, I assumed a sudden potential jump due to the different Fermi velocities on both

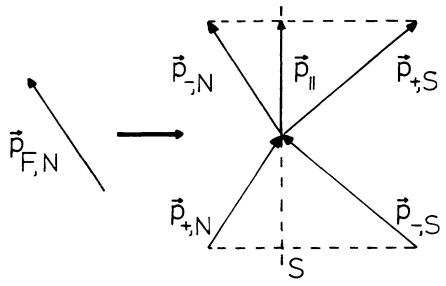

FIG. 2. Construction of the Fermi momenta that are mixed by the matching condition [Eqs. (2.5a)–(2.5e)].

sides and an additional δ potential at the interface. R_z is given by

$$R_z=[(v_{Nz}^*-v_{Sz}^*)^2+4V_s^2]/[(v_{Nz}^*+v_{Sz}^*)^2+4V_s^2] \tag{2.5e}$$

with

$$v_{kz}^*=v_{F,k}^*(\hat{\mathbf{p}}\cdot\hat{\mathbf{z}}) .$$

In this model, the usual assumption was made, that the (pseudo) wave functions of the corresponding effective-mass Hamiltonians and their first derivatives match continuously at the interface (see, for instance, Ref. 33).

The various momenta involved are shown in Fig. 2. The matching condition at $z=0$ mixes those propagators whose momentum directions lie along flight trajectories. To illustrate its use, suppose we start on the N side with a direction $\hat{\mathbf{p}}$ corresponding to a Fermi momentum $p_{F,N}\hat{\mathbf{p}}$. We then determine the parallel component $\mathbf{p}_{\parallel}=p_{F,N}(1-\hat{\mathbf{z}}\cdot\hat{\mathbf{p}})\hat{\mathbf{p}}$ and construct $\hat{\mathbf{p}}_{\pm,N}$ and $\hat{\mathbf{p}}_{\pm,S}$. For $p_{F,N}\neq p_{F,S}$, total reflection may occur depending on the angle of incidence. In these cases, the specular condition (2.4) must be applied at $z=0$.

The quasiclassical equation (2.3) together with the set of the boundary and matching conditions (2.4)–(2.5) and the normalization condition (2.2c) has finally been completed by the self-consistency equations for $\tilde{\Delta}_n(z)$ and $\tilde{\varepsilon}_n(z)$, which are, in the strong-coupling case, the local Eliashberg equations,

$$\tilde{\Delta}_n(z)=T\sum_m[\lambda(\varepsilon_n-\varepsilon_m,z)-\mu^*(z)] \times\int d\Omega_p(4\pi)^{-1}f(\hat{\mathbf{p}},z;\varepsilon_m) , \tag{2.6a}$$

$$i\tilde{\varepsilon}_n(z)=i\varepsilon_n-T\sum_m\lambda(\varepsilon_n-\varepsilon_m,z) \times\int d\Omega_p(4\pi)^{-1}g(\hat{\mathbf{p}},z;\varepsilon_m) , \tag{2.6b}$$

with

$$f(\hat{\mathbf{p}},z;\varepsilon_n)=\tfrac{1}{2}\,\mathrm{Tr}[\hat{g}(\hat{\mathbf{p}},z;\varepsilon_n)(\hat{\tau}_1-i\hat{\tau}_2)] , \tag{2.6c}$$

$$g(\hat{\mathbf{p}},z;\varepsilon_n)=\tfrac{1}{2}\,\mathrm{Tr}[\hat{g}(\hat{\mathbf{p}},z;\varepsilon_n)\hat{\tau}_3] , \tag{2.6d}$$

and

$$\lambda(\varepsilon_n-\varepsilon_m,z)=\int d\Omega\,\alpha^2F(\Omega,z)2\Omega/[(\varepsilon_n-\varepsilon_m)^2+\Omega^2] . \tag{2.6e}$$

In the weak-coupling limit, i.e., for $\tilde{\varepsilon}_n(z)=(1+\lambda)\varepsilon_n$, $\tilde{\Delta}_n(z)=(1+\lambda)\Delta(z)$, Eq. (2.6a) has the simpler form

$$\Delta(z)=T\sum_m g_{\mathrm{BCS}}(z)\int d\Omega_p(4\pi)^{-1}f(\hat{\mathbf{p}},z;\varepsilon_m) . \tag{2.7a}$$

The mass enhancement factor $(1+\lambda)$ is absorbed into the Bardeen-Cooper-Schrieffer–coupling constant and into a renormalized Fermi velocity $v_F^*=v_F/(1+\lambda)$ and thus disappears from the theory. The summation in (2.7a) has to be cut off at an energy of the order of the Debye energy. Using standard arguments, (2.7a) can be replaced by a form more suitable for numerical purposes:

$$\Delta(z)=\frac{2T\sum_n\int d\Omega_p(4\pi)^{-1}f(\hat{\mathbf{p}},z;\varepsilon_n)}{\ln[T/T_c(z)]+\sum_n 1/(n-0.5)} \tag{2.7b}$$

with

$$T_c(z)=\begin{cases}T_{cN}, & -a<z<0\\ T_{cS}, & 0<z .\end{cases} \tag{2.7c}$$

It is important to note that the summations in (2.7b) can already be cut off at an energy of, say, $10T_c$. In contrast to the conventional formulation,[25] the above stated form of the self-consistency equation is stable with respect to a simple iteration procedure. It was first published for p-wave superfluids in Ref. 34.

In the remainder of this section, I focus on the weak-coupling case, but a few strong-coupling results will be discussed in Sec. III.

With the above set of equations, the pair potential $\Delta(z)$ can be determined by an iterative procedure that needs only a few minutes (maximum) on a VAX-11 computer. For $\Delta(z)$ given, the local density of states, as measured by a tunneling experiment with specular tunneling characteristics, can be calculated by

$$N_T(E,-a)=-(1/2\pi) \times\mathrm{Im}\{\mathrm{Tr}[\hat{g}(\hat{\mathbf{p}}=\hat{\mathbf{z}},-a,-i(E+i0))]\} . \tag{2.8}$$

This is the simplest case. In general, the propagator in (2.8) is replaced by a (weighted) average over the possible momentum directions. The so-called random tunneling case, where all directions have equal weight, is most often quoted. Since I am primarily interested in the influence of the self-consistency on $N_T(E,-a)$, I restrict myself to a discussion of specular tunneling.

As a demonstration of the handiness of the quasiclassical equations, I now calculate the local density of states in the case of a steplike pair potential, i.e.,

$$\Delta(z)=\begin{cases}\Delta_N, & -a<z<0\\ \Delta_S, & 0<z .\end{cases} \tag{2.9}$$

In addition, an interface potential

$$V_{\mathrm{int}}(z)=V_s\delta(z) \tag{2.10}$$

simulates possible imperfections of the contact plane.

The differential equation (2.3a) can be easily solved in a region of constant pair potential and leads to the following solutions in the N and S regions:

$$\hat{g}_N(\hat{\mathbf{p}}_{\pm,N},z)=-(i\pi/\tilde{\Omega}_N)[A_1(\varepsilon_n\hat{\tau}_3-\Delta_N\hat{\tau}_2)+A_2(\Delta_N\hat{\tau}_3+\varepsilon_n\hat{\tau}_2\pm i\tilde{\Omega}_N\hat{\tau}_1)\exp(2\tilde{\Omega}_N z/v^*_{Nz})$$
$$+A_3(\Delta_N\hat{\tau}_3+\varepsilon_n\hat{\tau}_2\mp i\tilde{\Omega}_N\hat{\tau}_1)\exp(-2\tilde{\Omega}_N z/v^*_{Nz})] , \quad (2.11a)$$

$$\hat{g}_S(\hat{\mathbf{p}}_{\pm,S},z)=-(i\pi/\tilde{\Omega}_S)[(\varepsilon_n\hat{\tau}_3-\Delta_S\hat{\tau}_2)+D(\Delta_S\hat{\tau}_3+\varepsilon_n\hat{\tau}_2\mp i\tilde{\Omega}_S\hat{\tau}_1)\exp(-2\tilde{\Omega}_{Sz}/v^*_{Sz})] , \quad (2.11b)$$

with $\tilde{\Omega}_{N,S}=(\varepsilon_n^2+\Delta_{N,S}^2)^{1/2}$. $\hat{g}_N$ ($\hat{g}_S$) denotes the propagator in the region N (S).

The ansatz [Eqs. (2.11a) and (2.11b)] already includes the symmetry relation

$$\hat{g}(\hat{\mathbf{p}}_-,\mathbf{R};\varepsilon_n)=-\hat{g}^\dagger(-\hat{\mathbf{p}}_-,\mathbf{R};\varepsilon_n)=-\hat{g}^\dagger(\hat{\mathbf{p}}_+,\mathbf{R};\varepsilon_n)$$

as well as the fact that $\hat{g}_S$ has to be bounded everywhere and must be normalized. (The first equality is a general symmetry relation, and the second one is a consequence of the rotational invariance around the interface normal.) The four constants $A_{1,2,3}$ and D can now be directly calculated. Normalization of $\hat{g}_N$ implies

$$A_1^2=1-4A_2A_3 , \quad (2.12)$$

and the condition (2.4) leads to

$$A_3=A_2\exp(-4\tilde{\Omega}_N a/v^*_{Nz}) . \quad (2.13)$$

Use of the matching equations (2.5) yields immediately

$$D=A_3-A_2 \quad (2.14a)$$

and

$$\frac{1-R_z}{1+R_z}[A_1\varepsilon_n(\Delta_S-\Delta_N)+(A_2+A_3)(\varepsilon_n^2+\Delta_N\Delta_S)]=D . \quad (2.14b)$$

Inserting (2.13) in (2.14b), squaring and using (2.12), leads to

$$A_1=[1-R_zB^2+(B^2-R_z)\exp(-4\tilde{\Omega}_N a/v^*_{Nz})]/N , \quad (2.15a)$$

$$A_2=-iB(1-R_z)/N , \quad (2.15b)$$

$$A_3=A_2\exp(-4\tilde{\Omega}_N a/v^*_{Nz}) , \quad (2.15c)$$

$$D=A_3-A_2 , \quad (2.15d)$$

with the abbreviations

$$B=-i\varepsilon_n(\Delta_S-\Delta_N)/(\varepsilon_n^2+\tilde{\Omega}_N\tilde{\Omega}_S+\Delta_N\Delta_S) , \quad (2.16a)$$

$$N=\{[1-R_zB^2-(B^2-R_z)\exp(-4\tilde{\Omega}_N a/v^*_{Nz})]^2$$
$$-4R_z(1-B^2)^2\exp(-4\tilde{\Omega}_N a/v^*_{Nz})\}^{1/2} . \quad (2.16b)$$

In the squaring step, one loses the information on the sign of A_1, which is recovered by the requirement $A_1\to 1$ in the limit $a\to\infty$.

Having found the quasiclassical propagator, we can immediately calculate the local, direction-resolved tunneling density of states by an analytic continuation of the upper diagonal component of $\hat{g}$. Equation (2.9) leads to

$$N_T(E,\hat{\mathbf{p}},-a)=\mathrm{Im}[(E/\Omega_N)[i(1-R_z)(E^2-\Delta_N\Delta_S)\cos(2\Omega_N a/v^*_{Nz})$$
$$+(1+R_z)\Omega_N\Omega_S\sin(2\Omega_N a/v^*_{Nz})+i(1-R_z)\Delta_N(\Delta_S-\Delta_N)]$$
$$\times(\{[i(1-R_z)(E^2-\Delta_N\Delta_S)\sin(2\Omega_N a/v^*_{Nz})-(1+R_z)\Omega_N\Omega_S\cos(2\Omega_N a/v^*_{Nz})]^2-4R_z\Omega_N^2\Omega_S^2\}^{1/2})^{-1}] \quad (2.17)$$

with

$$\Omega_{N,S}=\begin{cases}(E^2-\Delta_{N,S}^2)^{1/2} & \text{for } E>\Delta_{N,S} ,\\ i(\Delta_{N,S}^2-E^2)^{1/2} & \text{for } E<\Delta_{N,S} .\end{cases}$$

This result is the same as has been obtained by a more involved calculation using microscopic Green's functions, and a subsequent averaging over terms oscillating with a phase $p_{F,N}a$ [see, e.g., Eq. (3.60) of Ref. 4]. In the next section, the tunneling density of states is calculated for the exact $\Delta(z)$, and the result is compared with (2.17).

III. NUMERICAL RESULTS

If the N layer is very thin compared to the coherence length, $\Delta(z)$ can be well described by a step function. This situation has been extensively investigated by Arnold,[9] who showed how to approximate the self-consistency equation in order to get the correct step height. I present calculations of the pair potential in the case of a medium or large film thickness, where $\Delta(z)$ devi-

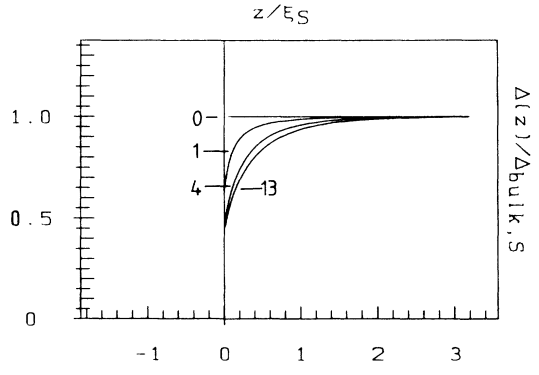

FIG. 3. Pair potential $\Delta(z)$; $T_{cN}=0$, $T=0.15$ $a=1.5$, $v_N=1$, $V_s=0$; different iteration steps: 0 (start), 1, 4, 13 (self-consistency).

ates appreciably from a step function. Subsequently, I discuss to what extent these deviations influence the tunneling density of states. For this purpose, $N_T(E)$ was calculated with the self-consistently determined pair potential, and the result was compared with the step approximation given by (2.17).

All variables needed are from now on given in units defined by the substrate as shown in the table below.

Variable	Unit
Temperature	T_{cS}
Energy	$1.76k_BT_{cS}$ [$=\Delta_{S,\text{bulk}}(T=0)$ in the weak-coupling case]
Velocity	v_S^*
Length	$\xi_S=v_S^*/3.52k_BT_{cS}$

Note, that ξ_S is not exactly the same as ξ_{prox}, which is usually used in the literature.[4] My choice of ξ_S facilitates the comparison of systems with different Fermi velocities.

For simplicity, the calculations assume equal effective masses on both sides. The case of different masses is discussed elsewhere[35] in connection with the heavy fermion systems. We therefore have as input parameters the thickness a, the Fermi velocity v_N^*, and the transition temperature T_{cN} of the N layer, the barrier strength V_s, and the temperature T.

Various steps of the iteration procedure for $\Delta(z)$ are shown in Fig. 3. After the first iteration, the pair potential is still far from self-consistency. The iteration procedure was terminated, if the Δ's at subsequent iterations differed by at most 0.01 at every point. Possible "creeping" of subsequent iterates could be avoided by the aid of an overrelaxation factor.

In the following calculations, T_{cN} has the value 0.13 corresponding to the combination Al/Nb (unless otherwise stated).

First, I want to discuss the influence of the layer thickness a. In Figs. 4(a)–4(c), examples with $a=0.1$, $a=1.5$, and $a=3.0$ are shown. The interface was assumed to be completely transparent ($v_N^*=1$, $V_s=0$), and the temperature $T=0.05$ was well below the transition temperatures of the two metals. In the first case ($a=0.1$), the pair potential of the N layer was enhanced over the whole region by a factor of 4 compared with the value of the bulk material (dashed line). For thicker N layers [Figs. 4(b) and 4(c)], the overall enhancement is not so dramatic, but still remarkable. The weakening of the pair potential on the S side depends, of course, on the layer thickness, but the influence saturates at thicknesses between one and two coherence lengths ξ_s. As a contrast to Fig. 4, a typical situation covered by the investigations of Arnold *et al.* is shown in Fig. 5 ($a=0.01$).

Of special interest is the situation of a temperature above the transition temperature T_{cN} of the layer, because in this case the superconducting state of N is induced by the substrate S and not merely enhanced. This can be seen in Fig. 6, where, except for T, the system parameters are the same as in Fig. 4(b). Again, the dashed line denotes the bulk value $\Delta_{\text{bulk},N}(T=0)$. There is practically no difference between the curve at $T=0.15$ and the one at $T=0.05$ in Fig. 4(b); the strong influence of the substrate effectively blocks the pair breaking in the N metal.

Let us now investigate the influence of a nonideal interface caused by an "electronic mismatch" ($v_N^*\neq 1$) and/or a nonzero interface potential V_s. In Fig. 7, several results with $v_N^*>1$ and $V_s=0$ are presented. The obvious "asymmetry" of the proximity effect in comparison to Fig. 4(b) stems from the fact that excitations attending the interface from the N side are totally reflected, if the angle of incidence (measured with respect to the interface normal) is too large. This implies a suppression of the proximity effect on the N side. In the extreme case $v_N^*=10$ the critical angle of incidence is about 6°, so that only 0.5% of the excitations transmit the interface and have the chance of being scattered by Andreev reflection. In Fig. 8 the situation is just reversed ($v_N^*<1$); total reflection occurs on the S side. The Fermi velocities were chosen in such a way that the reflection coefficient for normal incidence,

$$R_0=[(1-v_N^*)^2+V_s^2]/[(1+v_N^*)^2+V_s^2] \tag{3.1}$$

is the same as in Fig. 7.

This "asymmetric" feature is, of course, absent in the case $v_N^*=1$, $V_s\neq 0$, as shown in Fig. 9. The reflection coefficients are again the same as in the preceding two figures.

The self-consistently determined pair potential serves now as an input for the calculation of the tunneling density of states. It is of interest to know how large the results deviate from those computed under the assumption of a steplike pair potential [Eq. (2.17)]. I choose $\Delta_S=1$ and $\Delta_N=\Delta(z=-a)$ as parameters for the step approximation, where the value for $\Delta(z=-a)$ has been taken from the above self-consistent calculations. The results corresponding to Figs. 4(b) and 4(c) are shown in Figs. 10(a) and 10(b) ($T_{cN}=0.13$, $T=0.05$, $v_N^*=1$, $V_s=0$, $a=1.5$ and 3.0). The step approximation is plotted as a dashed line. The agreement with the numerical result is astonishingly good. The position of the bound state is practically unchanged compared with the exact calculation. The main difference is a phase shift in the McMillan-Rowell-Tomasch oscillations (which are of extremely long wavelength here) in the continuous part of the spectrum. We expect the strongest deviation, if N is an ideal normal material [$\Delta_N(z)\equiv 0$]; an example is shown in Fig. 11 [$\Delta(z)$ from Fig. 3]. In this case, the step approximation can still be improved by choosing a larger effective thickness $a_{\text{eff}}=1.65$ instead of $a=1.5$ (see Fig. 12).

In order to show more clearly the shift in the virtual bound states, an example with the larger layer thickness $a=4$ and $T_{cN}=0$ is presented in Fig. 13. Apart from the phase shift, the resonance structure dies out faster than in the step approximation.

All tunneling spectra presented so far have been calculated for systems with a fully transparent interface. In the partly transparent case, the proximity effect is reduced and $\Delta(z)$ becomes more steplike (cf. Figs. 7–9). In view of the above results, one does not expect an appreciable difference between the step approximation and the full numerical calculation. This can be seen for three different examples ($v_N^*=2$, $v_N^*=0.5$, and $V_S=0.7$) in Figs. 14, 15, and 16.

Finally, I want to present the results of a few strong-

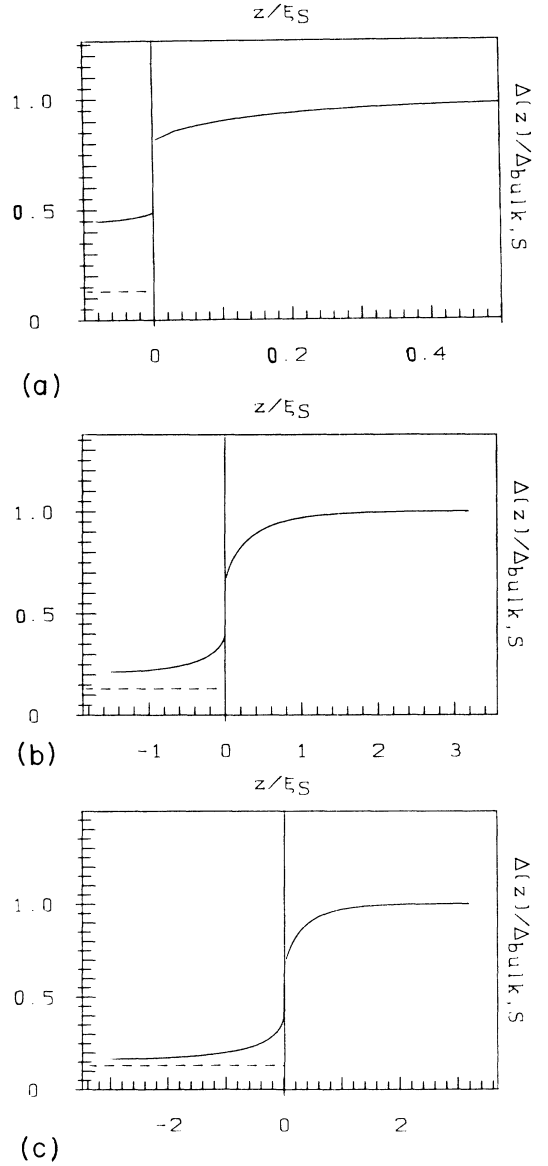

FIG. 4. Self-consistent pair potential $\Delta(z)$. $T_{cN}=0.13$, $T=0.05$, $v_N=1$, $V_s=0$; dashed line: $\Delta_{\text{bulk}}(T=0)$ of the N metal. (a) $a=0.1$; (b) $a=1.5$; (c) $a=3.0$.

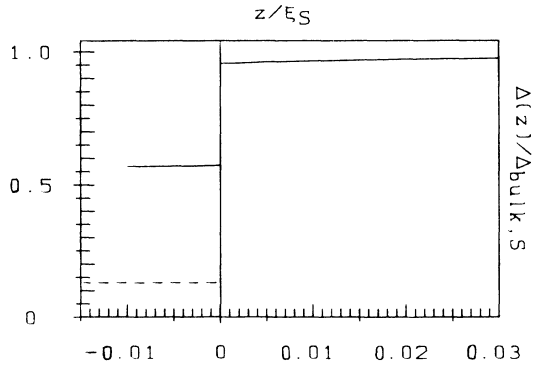

FIG. 5. Self-consistent pair potential $\Delta(z)$. $T_{cN}=0.13$, $T=0.05$, $a=0.01$, $v_N=1$, $V_s=0$; dashed line: $\Delta_{\text{bulk}}(T=0)$ of the N metal.

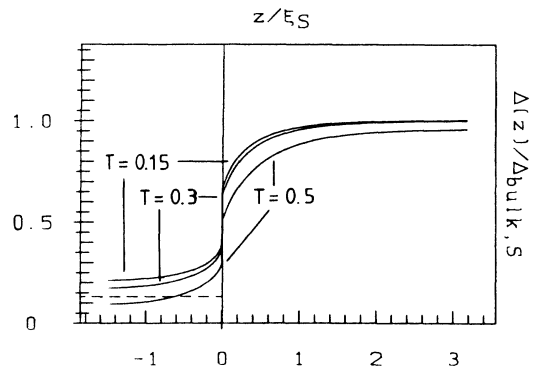

FIG. 6. Self-consistent pair potential $\Delta(z)$ at different temperatures; $T_{cN}=0.13$, $a=1.5$, $v_N=1$, $V_s=0$; dashed line: $\Delta_{\text{bulk}}(T=0)$ of the N metal.

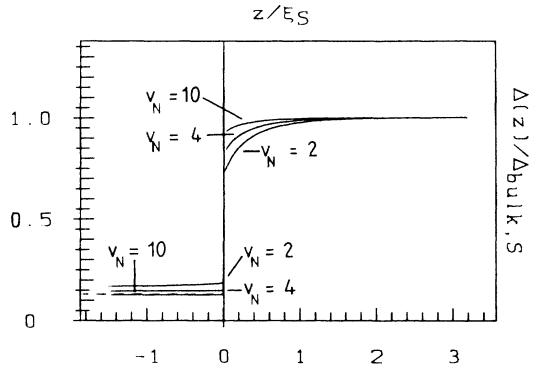

FIG. 7. Self-consistent pair potential $\Delta(z)$. $T_{cN}=0.13$, $T=0.05$, $a=1.5$, $V_s=0$; different $v_N>1$: $v_N=2$ ($R_0=0.11$), $v_N=4$ ($R_0=0.36$), $v_N=10$ ($R_0=0.67$); dashed line: $\Delta_{\text{bulk}}(T=0)$ of the N metal.

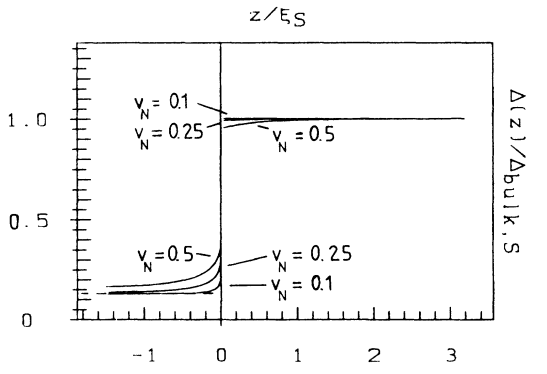

FIG. 8. Self-consistent pair potential $\Delta(z)$. $T_{cN}=0.13$, $T=0.05$, $a=1.5$, $V_s=0$; different $v_N<1$: $v_N=0.5$ ($R_0=0.11$), $v_N=0.25$ ($R_0=0.36$), $v_N=0.1$ ($R_0=0.67$); dashed line: $\Delta_{\text{bulk}}(T=0)$ of the N metal.

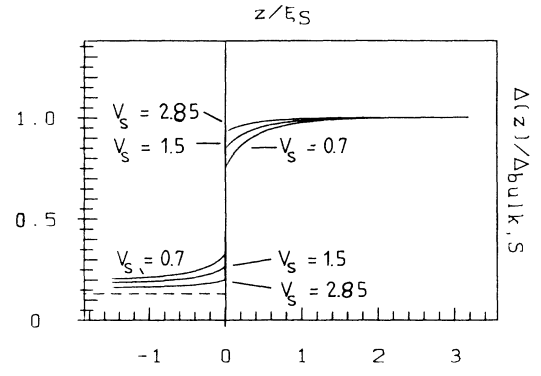

FIG 9. Self-consistent pair potential $\Delta(z)$. $T_{cN}=0.13$, $T=0.05$, $a=1.5$, $V_s=0$; different V_s: $V_s=0.7$ ($R_0=0.11$), $V_s=1.5$ ($R_0=0.36$), $V_s=2.85$ ($R_0=0.67$); dashed line: $\Delta_{\text{bulk}}(T=0)$ of the N metal.

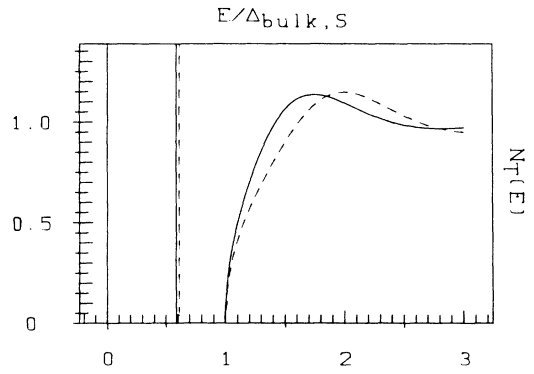

FIG. 11. Tunneling density of states; $\Delta(z)$ from Fig. 3. Step approximation with $a_{\text{eff}}=a=1.5$; $\Delta_N=0$.

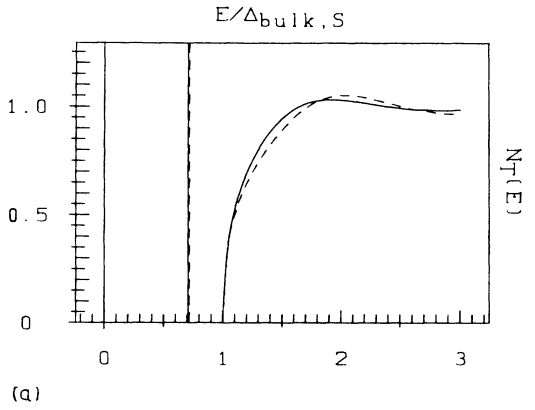

FIG. 10. Tunneling density of states; solid line: self-consistent $\Delta(z)$; dashed line: step approximation with parameters $\Delta_S=1$, Δ_N as given. (a) $\Delta(z)$ from Fig. 4(b); $\Delta_N=0.22$. (b) $\Delta(z)$ from Fig. 4(c); $\Delta_N=0.17$.

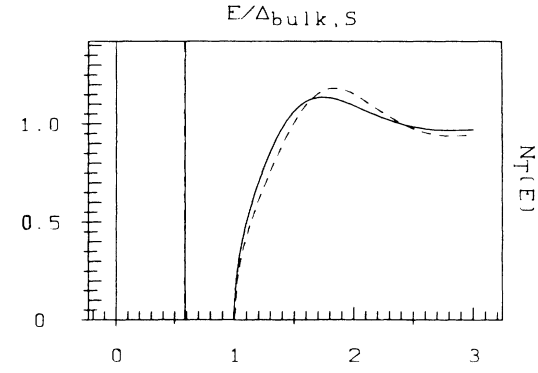

FIG. 12. Same as Fig. 11, but $a_{\text{eff}}=1.65$; $\Delta_N=0$.

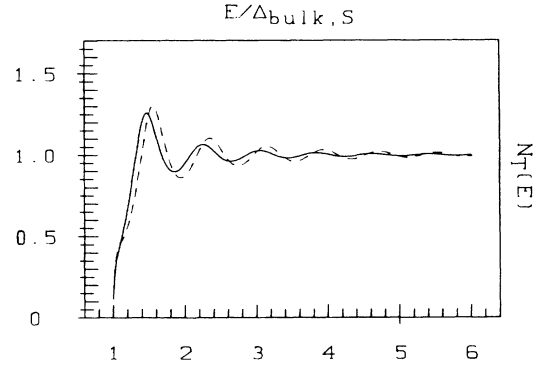

FIG. 13. McMillan-Rowell-Tomasch oscillations. ($T_{cN}=0$, $T=0.15$, $a=4$, $v_N=1$, $V_s=0$; $\Delta_N=0$).

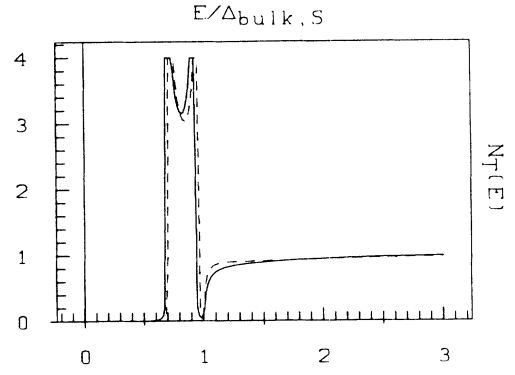

FIG. 14. Tunneling density of states; $\Delta(z)$ from Fig. 7 ($v_N=2$).

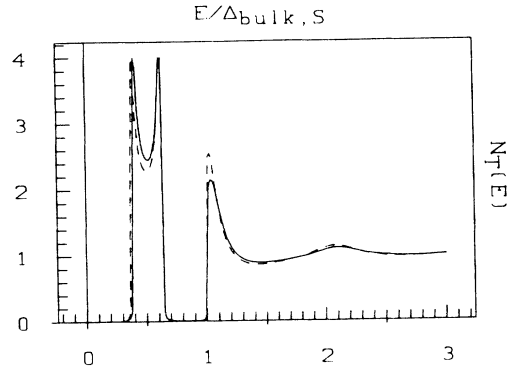

FIG. 15. Tunneling density of states; $\Delta(z)$ from Fig. 8 ($v_N=0.5$).

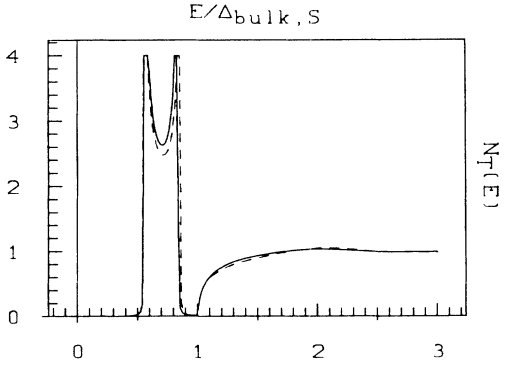

FIG. 16. Tunneling density of states; $\Delta(z)$ from Fig. 9 ($V_s=0.7$).

coupling calculations. To keep the discussion simplest, I chose a weak-coupling normal metal ($T_N=0$) for the N layer, and Pb (using the α^2F data tabulated in Ref. 36) for the S substrate. The interface was treated for simplicity as in Ref. 9, i.e., I assume equal Fermi momenta on both sides and perfect transmission of the quasiparticles. The

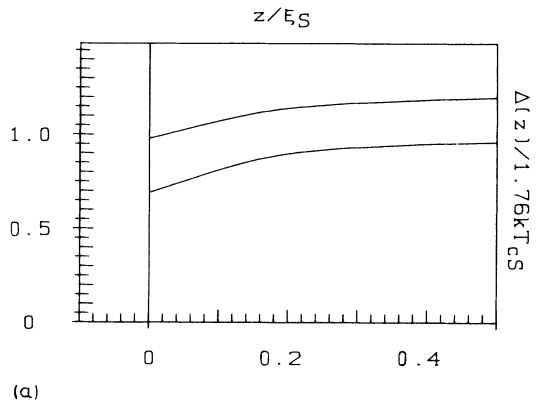

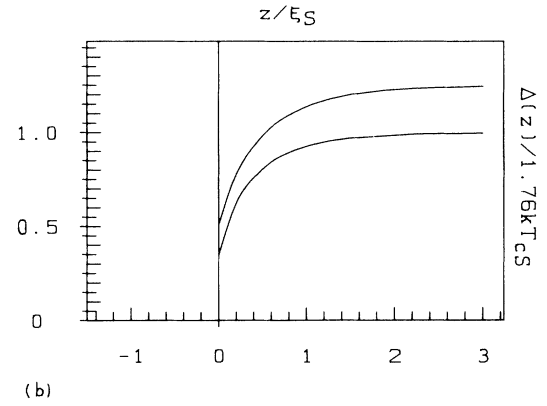

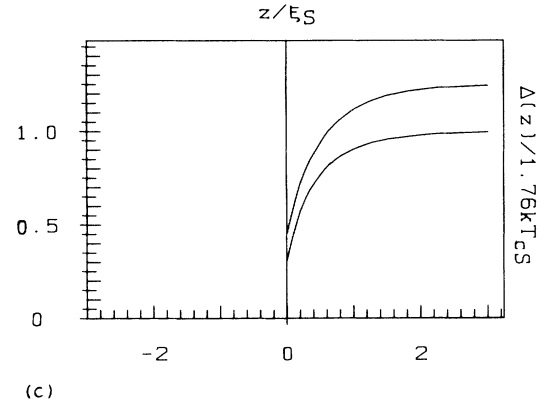

FIG. 17. Pair potential for a strong-coupling (upper curve) and the corresponding weak-coupling substrate (lower curve). The N layer is a weak-coupling normal metal. Parameters: $T_{c,N}=0$ K, $T_{c,S}=7.21$ K, $T=4$ K, $v_{F,N}/v_{F,S}=1+\lambda_{Pb}=2.55$. α^2F, μ_5^* from Ref. 36 for Pb. (a) $a=0.1$; (b) $a=1.5$; (c) $a=3.0$.

ratio of the dressed Fermi velocities was chosen with $v_{F,N}^*/v_{F,S}^* = 1+\lambda_{Pb}$, where the electron-phonon coupling constant λ_{Pb} had the value 1.55. The layer thickness varied between 0.1 and $3.0\xi_S$. The pair potential $\Delta(z)$ was defined as the extrapolation of $\tilde{\Delta}_n(z)/Z_n(z)$ $[Z_n(z)=\tilde{\varepsilon}_n(z)/\varepsilon_n]$ to zero energy. For bulk superconductors, these values agree very well with the energy gaps.[37] For comparison, the calculations were repeated in the weak-coupling formalism. The results are shown in Figs. 17(a)–17(c). The upper curves give the strong-coupling pair potential, and the lower ones are the weak-coupling results. Deep in the substrate, we just see the bulk strong-coupling enhancement of 25%. At the interface, I found a relative enhancement of more than 40%. It seems that the proximity effect is less effective in the strong-coupling case. This might be explained by the reduction in the coherence length with increasing Matsubara energies. Finally, I would like to point out the efficiency of the quasiclassical scheme: fully self-consistent calculations of $\Delta(z)$ as shown in Fig. 17, on a VAX 8600 computer, needed between 45 sec and 1.5 min in the strong-coupling case, and 8–15 sec in the weak-coupling limit.

IV. SUMMARY

Using the quasiclassical method, the pair potential of a system consisting of a layer of a normal or superconducting metal on top of a very thick superconducting substrate was determined in a self-consistent way. Subsequently, the tunneling density of states $N_T(E)$ was calculated (in the weak-coupling limit). The results show that a step ansatz for the pair potential reproduces the exact $N_T(E)$ very well, provided the step parameters are properly adjusted with the help of the correct self-consistent $\Delta(z)$. The main difference is a phase shift in the McMillan-Rowell-Tomasch oscillations.

In addition, results for strong-coupling pair potentials have been presented. The proximity effect seems to be weakened in comparison with the corresponding weak-coupling case.

ACKNOWLEDGMENTS

I would like to thank Professor D. Rainer for many discussions on this subject and a critical reading of the manuscript.

*Present address: Siemens AG, Unternehmensbereich Kommunikations und Datentechnik, K D ST DF, Otto-Hahn-Ring 6, D-8000 Munich 83, Federal Republic of Germany.

[1]G. Deutscher and P. G. DeGennes, *Superconductivity,* edited by R. D. Parks (Marcel Dekker, New York, 1969), Vol. 2.
[2]A. Gilabert, Ann. Phys. (Paris) **2**, 203 (1977).
[3]P. Nédellec, Ann. Phys. (Paris) **2**, 253 (1977).
[4]E. L. Wolf and G. B. Arnold, Phys. Rep. **91**, 31 (1982).
[5]D. S. Falk, Phys. Rev. **132**, 1576 (1963).
[6]W. L. McMillan, Phys. Rev. **175**, 559 (1968).
[7]T. Wolfram, Phys. Rev. **170**, 481 (1968).
[8]O. Entin-Wohlman, J. Low Temp. Phys. **27**, 777 (1977).
[9]G. B. Arnold, Phys. Rev. B **18**, 1076 (1978).
[10]O. Entin-Wohlman and J. Bar-Sagi, Phys. Rev. B **18**, 3174 (1978).
[11]W. J. Gallagher, Phys. Rev. B **22**, 1233 (1980).
[12]W. J. Tomasch, Phys. Rev. Lett. **15**, 672 (1965).
[13]J. M. Rowell and W. L. McMillan, Phys. Rev. Lett. **16**, 453 (1966).
[14]L. Wong, S. Shih, and W. J. Tomasch, Phys. Rev. B **23**, 5775 (1981).
[15]S. Shih, Z. G. Kim, G. B. Arnold, and W. J. Tomasch, Phys. Rev. B **24**, 6440 (1981).
[16]R. Delesclefs and Ø. Fischer, J. Low Temp. Phys. **53**, 399 (1983).
[17]P. M. Chaikin and P. K. Hansma, Phys. Rev. Lett. **36**, 1552 (1976).
[18]G. B. Arnold, J. Zasadzinski, J. W. Osmun, and E. L. Wolf, J. Low Temp. Phys. **40**, 225 (1980).
[19]E. L. Wolf, J. Zasadzinski, J. W. Osmun, and G. B. Arnold, J. Low Temp. Phys. **40**, 19 (1980).
[20]E. L. Wolf, D. M. Burnell, Z. G. Khim, and R. J. Noer, J. Low Temp. Phys. **44**, 89 (1981).
[21]J. Zasadzinski, D. M. Burnell, E. L. Wolf, and G. B. Arnold, Phys. Rev. B **25**, 1622 (1982).
[22]D. M. Burnell and E. L. Wolf, J. Low Temp. Phys. **58**, 61 (1984).
[23]J. A. X. Alexander, T. P. Orlando, D. Rainer, and P. Tedrow, Phys. Rev. B **31**, 5811 (1985).
[24]F. J. Culetto, G. Kieselmann, and D. Rainer, in *Proceedings of the 17th International Conference on Low Temperature Physics, 1984,* edited by U. Eckern, A. Schmid, W. Weber, and H. Wühl (North-Holland, Amsterdam, 1984).
[25]G. Eilenberger, Z. Phys. **214**, 195 (1968).
[26]A. I. Larkin and Yu. N. Ovchinnikov, Zh. Eksp. Teor. Fiz. **55**, 2262 (1968) [Sov. Phys—JETP **28**, 1200 (1969)].
[27]J. W. Serene and D. Rainer, Phys. Rep. **101**, 221 (1983).
[28]A. L. Shelankov, J. Low Temp. Phys. **60**, 29 (1985).
[29]I. O. Kulik and A. N. Omel'yanchuk, Fiz. Nizk. Temp. **4**, 296 (1978) [Sov. J. Low Temp. Phys. **4**, 142 (1978)].
[30]L. J. Buchholtz and D. Rainer, Z. Phys. B **35**, 151 (1979).
[31]A. V. Zaitsev, Zh. Eksp. Teor. Fiz. **86**, 1742 (1984) [Sov. Phys.—JETP **59**, 1015 (1984)].
[32]G. Kieselmann, Ph.D. thesis, University of Bayreuth, 1985.
[33]E. W. Fenton, Solid State Commun. **54**, 709 (1985).
[34]W. Zhang, J. Kurkijärvi, and E. V. Thuneberg, Phys. Lett. **109A**, 238 (1985).
[35]B. Ashauer, G. Kieselmann, and D. Rainer, J. Low Temp. Phys. **63**, 349 (1986).
[36]J. M. Rowell, W. L. McMillan, and R. C. Dynes (private communication).
[37]D. Rainer, Physica **109&110B**, 1671 (1982).